WISCONSIN

UC-20,f

UNIVERSITY OF WISCONSIN • MADISON, WISCONSIN

PLASMA PHYSICS

CROSS FIELD DIFFUSION AND FLUCTUATION SPECTRA IN A LEVITATED OCTUPOLE IN THE PRESENCE OF A TOROIDAL FIELD

A.B. Ehrhardt[a], H.R. Garner, G.A. Navratil[b], R.S. Post

DOE/ET53051/14

November 1980

Printed in the United States of America
Available from
National Technical Information Service
U.S. Department of Commerce
5285 Port Royal Road
Springfield, VA 22161

NTIS Price codes
Printed copy: A02
Microfiche copy: A01

CROSS FIELD DIFFUSION AND FLUCTUATION SPECTRA

IN A LEVITATED OCTUPOLE IN THE PRESENCE OF A TOROIDAL FIELD

A.B. Ehrhardt[a)], H.R. Garner, G.A. Navratil[b)], R.S. Post

University of Wisconsin

Madison, Wisc. 53706

Abstract

The diffusion coefficient, $D_\perp$, for a collisionless hydrogen plasma was measured in the Levitated Octupole when a weak toroidal field was added. A 20-fold decrease in the anomalous diffusion was observed with $B_T/B_P \simeq 0.1$. Since the plasma is collisionless locally trapped particles in the poloidal field mirrors allows the convective cell activity (f < 600 Hz) to persist even when toroidal field was added. A shift in the $k_\perp$ spectrum to shorter wavelengths was noted. Measurments and calculations indicate that the higher frequency portion of the spectrum (f > 600 Hz) cannot be responsible for the observed diffusion.

CROSS FIELD DIFFUSION AND FLUCTUATION SPECTRA IN A LEVITATED OCTUPOLE IN THE PRESENCE OF A TOROIDAL FIELD

A.B. Ehrhardt[a], H.R. Garner, G.A. Navratil[b], R.S. Post

University of Wisconsin

Madison, Wisc. 53706

Introduction

Previous work describing the observed scaling of the cross-field particle diffusion coefficient, $D_\perp$, with density and magnetic field in the Wisconsin Levitated Octupole has explored both the collisional[1] (mean-free-path less than the connection length) and highly collisionless[2] regimes with a purely poloidal multipole field geometry. The collisional regime was investigated using sheared magnetic fields[3] (a toroidal magnetic field added to the multipole field) and purely poloidal multipole fields. In this paper we complete our survey of the diffusion coefficient scaling by reporting the effects of a sheared magnetic field on the diffusion in a highly collisionless plasma.

The work presented in Ref. 1-3 showed that the observed diffusion was caused by vortex modes or convective cell activity in the plasma. The observed scaling of the diffusion agreed with 1-dimensional vortex theory with a finite dielectric constant.[4] The level of this convective turbulence was greatly enhanced over the thermal levels and was produced by the turbulent gun injection process used to produce the confined plasma. In this paper we will present data showing the case of a collisionless plasma, when a very weak toroidal field was addeded ($B_T/B_P \lesssim 10^{-1}$).

All of the results presented here were obtained with the internal rings "levitated", i.e., no ring supports were present in the confined plasma volume. This was critically important when B_T was added. The change over from closed poloidal field lines to open field lines and flux surfaces allows substantial parallel flow of plasma to the supports influencing both the decay time and density profile shape. The hydrogen plasma was created by gun injection into a power crowbarred magnetic field exponentially decaying with time constant ~ 200 msec. Since the maximum time the rings are fully levitated is 20 msec all the data presented was taken within 20 msec after injection. Intitial densities were as high as 10^{10} cm^{-3} and could be reduced by partial obstruction of the injected plasma beam to 10^9 cm^{-3}. Ion temperatures ranged from 20 eV at early times to 5 eV, 20 msec after injection. The electron temperature ranged from 30 eV to 5 eV over the same time interval. When parameters of density or B were varied, observation times were chosen so as to keep both T_e and T_i constant.

Experimental Results

As described in Ref. 2 and 5, an interdigitated striped particle collector is mounted on the surface of an internal ring and measures the flux of plasma to the ring surface as a function of time. By using Langmuir probes calibrated with a microwave interferometer to measure the density profile near the ring surface, a diffusion coefficient can be caluclated: $D_\perp = \frac{\Gamma_\perp}{\nabla n}$ where $\Gamma_\perp$ is the flux of particles. By varying the density and magnetic field, the scaling of $D_\perp$ with these parameters can then be determined.

All of the results reported here were taken in the absolute-minimum-B region which extends from the ring surface out to the density peak. The density peak is located inside the separatrix, ψ_S. Shown in Figure 1 is the measured diffusion coefficient to the ring surface for fixed density, $n = 6 \times 10^9$ cm^{-3}, and $B_P = 1.0$ kG and varying B_T from 0 to 300 G. The magnitude of $D_\perp$ was halved by the addition of only 20 G of toroidal field (or $B_T/B_P \sim 10^{-2}$). The value of $D_\perp$ was then reduced to approximately $\frac{1}{20}$ of its $B_T = 0$ value when B_T was increased to 100 G. Further increases in B_T to 300 G produced no change in $D_\perp$ within the uncertainty in the measurement. The electron and ion temperatures at the time of these measurements were $T_i \sim 9$ eV and $T_e \sim 5$ eV.

With the fixed values of $B_P = 1$ kG and $B_T = 300$ G the density was varied from 10^9 cm^{-3} to almost 10^{10} cm^{-3}. The results are shown in Figure 2 and compared with calculated n^{-1} dependence of $D_\perp$. Additionally, the observed profile shape was compared with the shape predicted by a one-dimensional diffusion equation[6] and found to fit best by $D_\perp \propto 1/n$.[7] The B-independence of $D_\perp$ was verified by fixing the ratio $B_T/B_P = 0.24$ and the density varying B as shown in Fig. 3. The value of $D_\perp$ was found to be independent of $|B|$ over a factor of 3 range.

Fluctuation Spectrum Measurements

In order to determine the sources for the anomalous transport we have measured the fluctuation spectrum by two means. A movable cart which can scan the local value of the floating potential at all values of and was used to examine the very low frequency, long wavelength part of the spectrum ($0 < f < 1$ kHz). Higher frequency shorter wavelength fluctuations were examined using Langmuir probes at fixed locations. We first present the very low frequency measurements followed by the high frequency spectra.

For completeness we show the cell structure without toroidal field, Figure 4, as well as the new data on the effect of B_T, Figure 5. The average value of B_p for this data is 1 kG and the plasma density at $\psi = 5.5$ is $n = 10^9\ cm^{-3}$. Contours of constant floating potential are plotted as a function of the toroidal angle, θ, and the flux function, ψ. The data ia accumulated on a shot to shot basis with the total cell plot generated from several hundred shots. Only shots which were reproducible to $\pm$ 10% in ion saturation current monitored on the separatrix were used.

With the application of the toroidal field the initial plasma parameters n, T_e, and T_i remained the same but the resultant convective cell patterns are modified. (See Figure 5). The density gradient maximizes at $\psi = 4.0$. The region to which the diffusion measurements pertain is from $\psi = 2.2$ to the density maximum. Comparing Figure 4 and Figure 5, the long wave length portion of the spectrum was replaced by a shorter wave length spectrum. The potential amplitude was of the same magnitude in both cases. In order to estimate the effect of of convective cell spectrum on diffusion it is necessary to know how these floating potentials are distributed along a flux surface. The cart used to take the data for the cell plots has access only to the low field side of the ring. In order to measure the potential in the high field region between the ring and the vacuum wall, a probe was inserted into a fixed aximuthal location. By comparing the cell plots at two times, e.g., 5 msec and 20 msec, one can see that there are temporal potential variations with frequencies less than 600 Hz. When this portion of the spectrum was compared using probes located on the same surface but on the opposite side of the internal ring, we find that fluctuations are nearly identical in absence of B_T. With B_T = 300 G, the low frequency fluctuations are larger on the low field side of the ring where particles are mirror trapped then in the high field region. Thus we see that the convective cells aquire a finite $k_\perp$ for the $B_T \gtrsim 300$ G cases.

We have also measured the higher frequency portion 600 Hz < f < 10 kHz of the spectrum, and its dependence on toroidal field. The fluctuation data was taken by digitizing the signal from a Langmuir probe whose bandwith was set from 600 Hz to 10 kHz. The probe was located at $\psi = 4.0$ (point of maximum ∇n) behind and in front of the lower outer ring. Digitizing was started at 5 msec after gun injection. The eight bit by 1024 bin high speed A to D's were used to take data for 5 msec, allowing for measurements down to 200 Hz. The digitizing signal was then processed using a fast Fourier transform program. The FFT was relatively calibrated by analyzing digitized square waves whose Fourier components are known. The FFT was absolutely calibrated on a shot to shot basis using a frequency component easily identified from the raw data. The digitized signal was also played back into electronic spectrum analyzer yielding good agreement with the FFT. The data presented is $P(f) = P(\frac{\omega}{2\pi})$ where P(f) is power spectrum. It is formed in such a way that the total power in all modes is P_T

$$P_T = \int_0^\infty P(\omega)d\omega$$

$P(\omega)$ was calculated by transforming the floating potential $\tilde{\phi}(t)$ after removing any linear trends:

$$\phi(\omega) = \int_{\Delta t} \tilde{\phi}(t)e^{-i\omega t}dt$$

A periodigram of the Fourier coefficients was formed: $\phi(f)^2$ vs. f. This was smoothed and multiplied by bin width; i.e., the frequency window $\Delta f = 200$ Hz. The results are given in Figures 6 and 7.

The power spectra was found to peak at the lowest frequency measured (600 Hz). When the high frequency portion of the spectrum is compared using probes on the high field side of the rings to the low field side we find that $\int P(f)df$ to be the same in the absence of B_T. With $B_T = 300$ G, the high frequency flucutations (f > 600 Hz) are smaller on the low field side of the ring where B_T/B_P is maximized on the flux surface.

For 600 Hz $\leq$ f < 10 kHz corresponding to the drift wave frequency range fluctuations on the high field (front) of internal rings were found to have perpendicular wavelengths between 5 cm and 10 cm. That is $.1 \leq k_\perp \rho_i < .2$.

Discussion

In previous work[1-3] along with a recent publication[12] the very low frequency part of the fluctuation spectrum or convecitve cells have been shown to be responsible for the observed levels of anomalous diffusion. In the present experiments the addition of the toroidal field results in a decrease in the diffusion by a factor of 20 to approximately 40 cm^2/sec. For a purely poloidal case we have used the diffusion coefficient of Taylor and McNamara[8] to calculate $D_\perp = \frac{c^2 E_k^2}{B^2 k^2}(\exp(-k^2 D_\perp t)-1)$ from the measured E_k^2. We find that we are able to compute $D_\perp$ to within a small numerical factor of the measured $D_\perp$ using this method.[12,15] Although we do not have a 360° scan of the convective cell spectrum for the present case with 300 g, we can see qualitatively that the energy is concentrated shorter wavelength modes. Due to the strong $k_\perp$ dependence of $D_\perp$, only the longest wavelengths make significant contributions to the diffusion. Thus we see that the spectrum of Figure 5 will produce significantly less diffusion than that obtained from the spectrum of Fig. 4 consistent with the observations. In addition the flux surface averaged diffusion coefficient is reduced ~ 2 over the $B_T = 0$ case due to the localization of the convective cells in the low field region. Thus we conclude that the convective cell spectrum is primarily responsible for the crossfield transport. The diffusion expected from vortices of this type was invesitgated both theoretically and in simulation studies by Kamimura and Dawson[11] and found to scale as $D_\perp \alpha n^{-1}$ and independent of $|B|$ when the low frequency dielectric constant is included in agreement with the measured scaling of $D_\perp$ when $D_\perp = \frac{c^2}{B^2} E_k^2 \tau_k$ or $D_\perp = \frac{c^2}{B^2 \varepsilon_\perp} T_k^* \tau_k$. Where T_k^* is the effective temperature of the k mode and $\varepsilon_\perp$ is the low frequency dielectric constant. The correlation time τ_k is assumed to have an inverse n dependence; e.g, Coulomb collisions. Since these modes should damp by parallel ion diffusion τ_k is assumed to scale as $\tau_k \sim \tau_{ii}$, the ion-ion collision time. In these experiments $\tau_{ii} \sim 20$ msec initially. After 15 msec the ions have cooled by charge exchange to 5 eV while n decreases by 2 over this interval. Thus at t = 15 msec τ_{ii} is ~ 2 msec. In spite of this, the convective cell spectrum and anomalous diffusion persist. Thus it is necessary to invoke a driving mechanism for the convective cells.

A possible mechanism for driving the convective cells is the nonlinear coupling to drift waves as proposed by Cheng and Okuda.[12] However, in addition we note that due to the $E_{\parallel}$ caused by the finite resistivity of the current carrying conductors a current flows in the plasma. In this low density plasma the current is sufficient to drive the ion cyclotron mode[14] unstable as previously noted.[7]

We now consider the contribution of the high frequency part of the fluctuation spectrum (f > 600 Hz) to the cross-field transport. The perpendicular diffusion coefficient can be estimated by

$$D_{\perp} \sim \frac{\Gamma_{\perp}}{|\nabla n|} = \frac{\langle n\ V \rangle}{|\nabla n|} = \frac{1}{B}\ \frac{(n/\nabla n)}{kT_e/e} \int P(f)df$$

assuming optimum phase shift for maximum transport for every frequency component. Using the measured power spectrum P(f) shown in Figures 6 and 7 we conclude that for any value of B_T the high frequency modes can account for at most 20% of the observed transport as shown in Figure 1. Only the low frequency part of the spectrum (f < 600 Hz) has sufficient amplitude to account for the remainder of the transport.

All power spectra shown here are fluctuating potential measurements with $\frac{\tilde{\phi}}{kT_e/e} \sim 2\%$ for f < 600 Hz. The power spectra of the density fluctuations are not shown because $\frac{\Delta n}{n} \ll \frac{\tilde{\phi}}{kT_e/e}$ for low frequencies and cannot be measured by the techniques employed. For $f > 600$ Hz: $\frac{\Delta n}{n} \sim \frac{\tilde{\phi}}{kT_e/e} \sim 1\%$ for $B_T = 0$.

Conclusion

We have presented data which show that the addition of a weak toroidal field ($B_T/B_P \gtrsim 0.1$) significantly reduces the magnitude of the anomalous vortex diffusion. Observed values of the anamolous diffusion are as low as $\frac{1}{1000}$ of the Bohm value and are comparable with the best confinement results obtained in collisionless plasmas in other multipole experiments such as FM-1[9] and the G.A. dc Octupole.[10] However, the reduced value of $D_\perp$ obtained was still 100 times larger than the classical value for peak density of 10^{10} cm^{-3}. An examination of the potential structure in the plasma revealed the continued presence of convective cells but no fluctuations in the drift mode frequency range which which are large enough to directly cause the diffusion. Therefore we conclude that the convective cells must be responsible for the residual level of anamalous diffusion.

Earlier work showed that if the plasma is collisional (no trapped particles), the addition of a toroidal field ($B_T/B_P \sim 0.1$) eliminated the anomalous diffusion and only classical diffusion is observed.[3] When the plasma is collisionless the presence of excess charge trapped in the local poloidal field mirrors allows the convective cells to exist even in the presence of shear. Observations of the low frequency convective cell structures in the plasma showed an increase in the large $k_\perp$ number part of the spectrum with most of the amplitude in the lowest field portion of the local poloidal field mirrors. The region of largest convective cell activity occurs when the trapped particle population is the largest, as expected. The 20-fold decrease in the anomalous diffusion could then be caused by a localization of the convection to only a part of the flux surface coupled with a shift in the $k_\perp$ -spectrum to shorter wavelengths which are expected to cause less diffusion.[11]

There is nothing in our observations or theory which would preclude the existence of these modes in other toroidal machines such as bumpy tori or tokamaks. The observation that $\frac{\Delta n}{n} \ll \frac{\tilde{\phi}}{kT_e/e}$ for the convective cell spectra would imply that a search for these modes in other devices where the high temperature and density prevent the use of Langmuir probes to make a local potential measurement would be difficult. More sophisticated methods to measure the local value of space potential would have to be employed such as heavy ion beam probes.

Acknowledgement

We would like to acknowledge the many useful discussions with D.W. Kerst. We would like to point out that Jim Greenwood first confirmed the 1/n scaling of the diffusion coefficient from the shape of the density profile[16]. This work was performed under D.O.E. contract.

[a]Present address: Applied Physics Laboratories, Inc., John Hopkins Road, Laurel, MD 20810.

[b]Present address: Columbia Plasma Physics Laboratory, Columbia University, NY, NY 10027.

[1]G.A. Navratil, R.S. Post, and A.B. Ehrhardt, Phys. Fluids 20, 156 (1977).

[2]J.R. Drake, J.R. Greenwood, G.A. Navratil, and R.S. Post, Phys. Fluids 20, 148 (1977).

[3]G.A. Navratil, R.S. Post, and A.B. Ehrhardt, Phys. Fluids 22, 241 (1979).

[4]H. Okuda and J.M. Dawson, Phys. Fluids 16, 408 (1973).

[5]A. Cavallo, Phys. Fluids 19, 394 (1976).

[6]J.R. Drake and J.G. Berryman, Phys. Fluids 20, 851 (1977).

[7]J.R. Drake, D.W. Kerst, G.A. Navratil, R.S. Post, S. Ejima, R. LaHaye, C.P. Moeler, T. Ohkawa, P.I. Petersen, R. Prater, and S.K. Wong, Plasma Physics and Controlled Nuclear Fusion Research, Vol. II, ISEA, Vienna, 333 (1976).

[8]J.B. Tayler and B. McNamara, Phys. Fluids 14, 1482 (1971). Also see: Y. Salu and D. Montgomery, Phys. Fluids 20, 1 (1977).

[9]J. Sinnis, M. Okabayaski, J. Schmidt, and S. Yoshikawa, Phys. Rev. Lett. 29, 1214 (1972).

[10]R. Prater, S. Ejima, T. Ohkawa, and S.K. Wong, Phys. Fluids 21, 434 (1978).

[11]T. Kamimura and J.M. Dawson, Phys. Rev. Lett. 36, 313 (1976).

[12]A. Butcher Eharhardt and R.S. Post, submitted for publication.

[13] C.Z. Cheng and H. Okuda, Nuclear Fusion 18, 587 (1978).

[14] W.E. Drummand and M.N. Rosenbluth Phys. of Fluids 5, 1507 (1962).

[15] A. Butcher Ehrhardt, Ph.D. Thesis, University of Wisconsin, 1979.

[16] J. Greenwood, Ph.D. Thesis, University of Wisconsin, 1975.

FIGURE CAPTIONS

Fig. 1 Measured values of perpendicular diffusion coefficient, $D_\perp$ (ψ=4), as a function of toroidal field at ψ = 4.

Fig. 2 Measured $D_\perp$ (ψ=4) as a function of density showing its 1/n dependence.

Fig. 3 Measured $D_\perp$ (ψ=4) as a function of B_P showing its independence of B .

Fig. 4 Cell plot for B_T = 0 showing lines of constant potential (volts) in the toroidal direction, θ, versus the poloidal flux function, ψ. The poloidal field gap is at $\theta = 0^o$. The internal ring surface is located at ψ = 2.2 and the ψ_S = 5.7. The times shown are referenced to the injection time.

Fig. 5 Same as Figure 4 except B_T = 300 G.

Fig. 6 Power spectra of fluctuations in the frequency range 600 Hz to 10 kHz on the high field side of the ring (front) are shown for the values of B_T.

Fig. 7 Power spectra obtained as in Figure 6 for the low field side of the ring (behind).

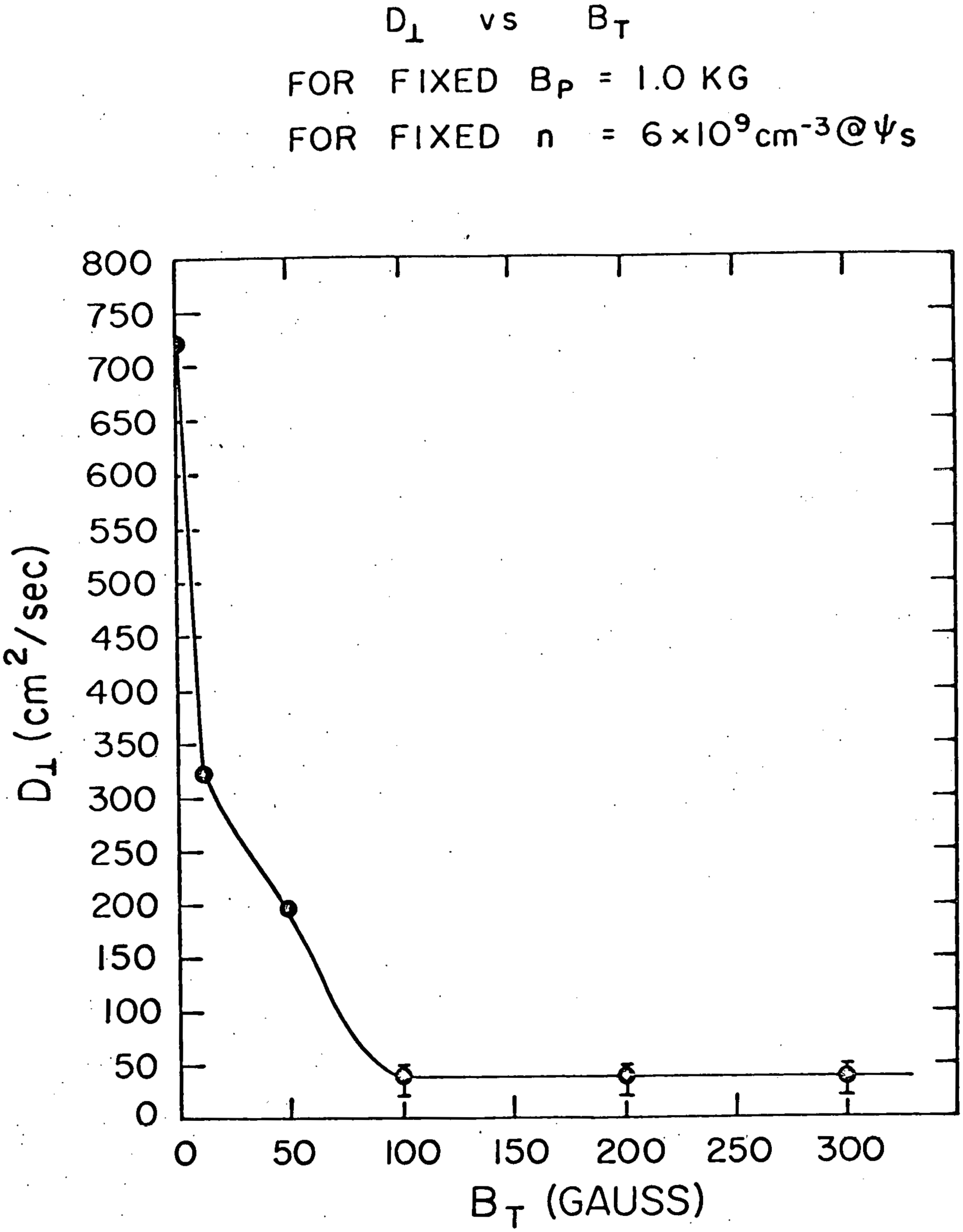
D⊥ vs B_T
FOR FIXED B_P = 1.0 KG
FOR FIXED n = 6×10^9 cm^-3 @ψs
800
750
700
650
600
550
500
450
400
350
300
250
200
150
100
50
0
D⊥ (cm²/sec)
0
50
100
150
200
250
300
B_T (GAUSS)

Fig. 1

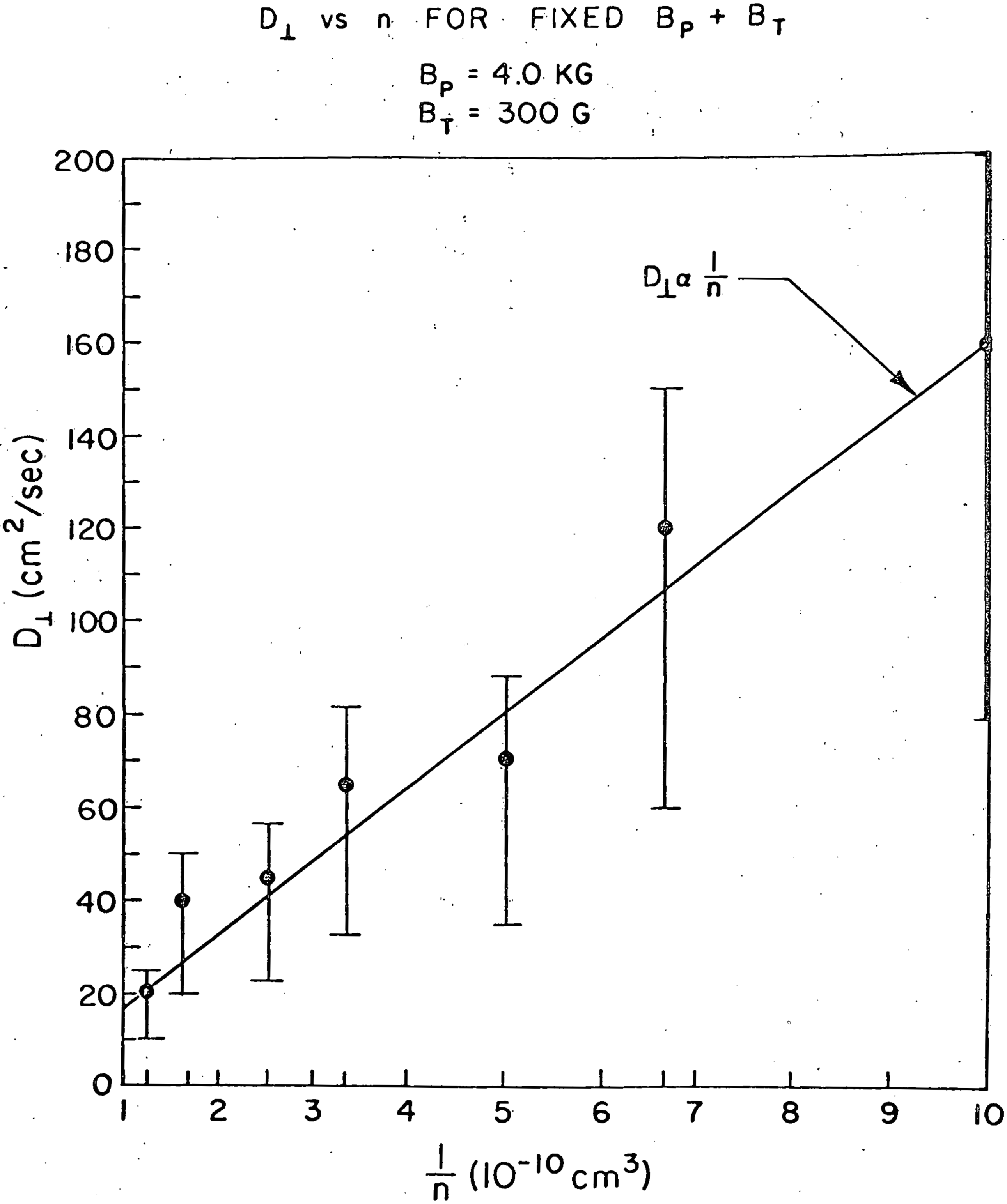

D⊥ vs n FOR FIXED B P + B T
B P = 4.0 KG
B T = 300 G
D⊥ α 1/n
D⊥ (cm²/sec)
200
180
160
140
120
100
80
60
40
20
0
1
2
3
4
5
6
7
8
9
10
1/n (10⁻¹⁰ cm³)

Fig. 2

FIXED $\frac{B_T}{B_P} = 0.24$ AND FIXED $n = 3 \times 10^9\ cm^{-3}$

VARY |B|

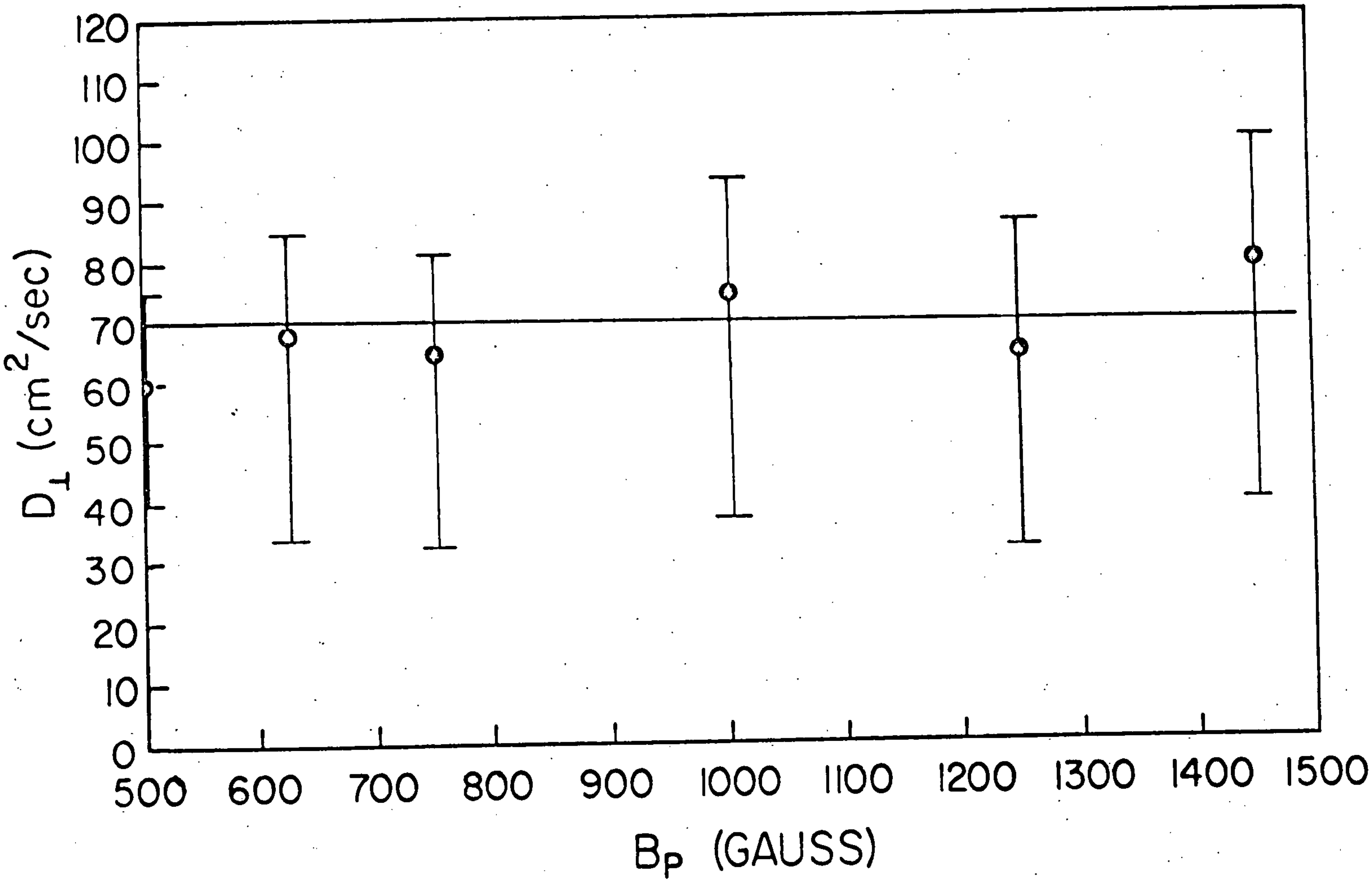

Fig. 3

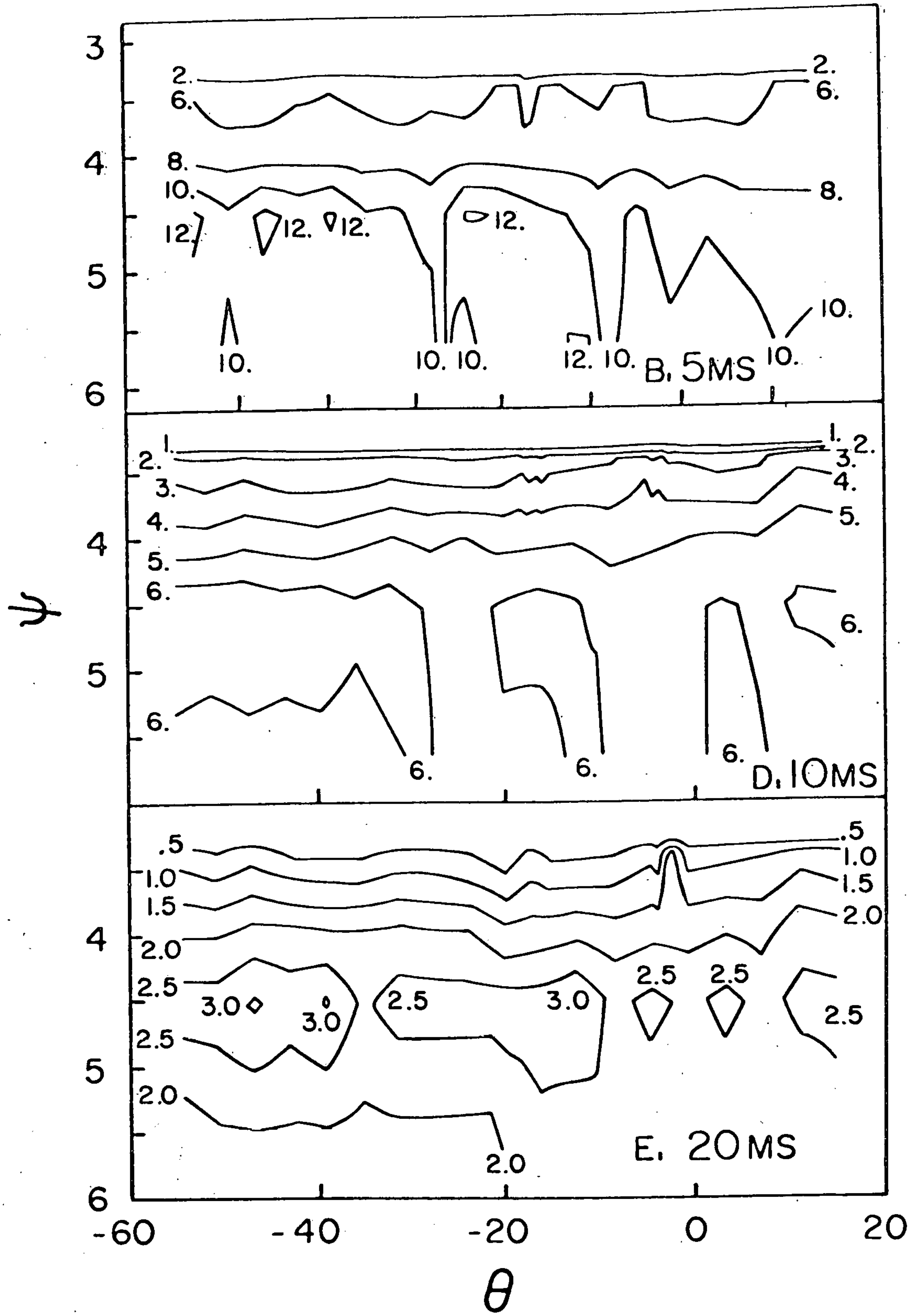

3
4
5
6
2.
6.
8.
10.
12.
10.
B. 5MS
ψ
1.
2.
3.
4.
5.
6.
D. 10MS
.5
1.0
1.5
2.0
2.5
3.0
E. 20MS
-60
-40
-20
0
20
θ

Fig. 4

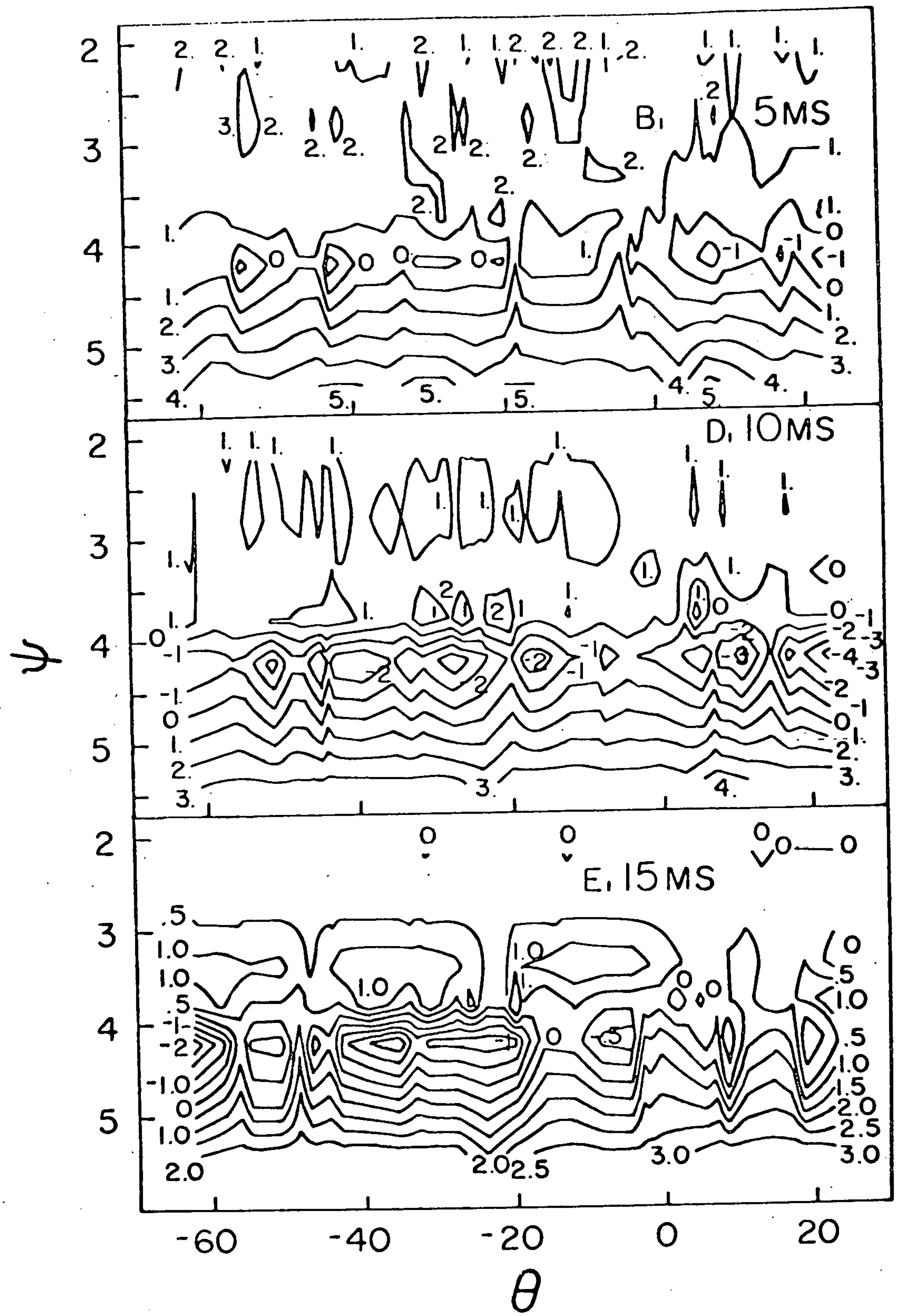

Fig. 5

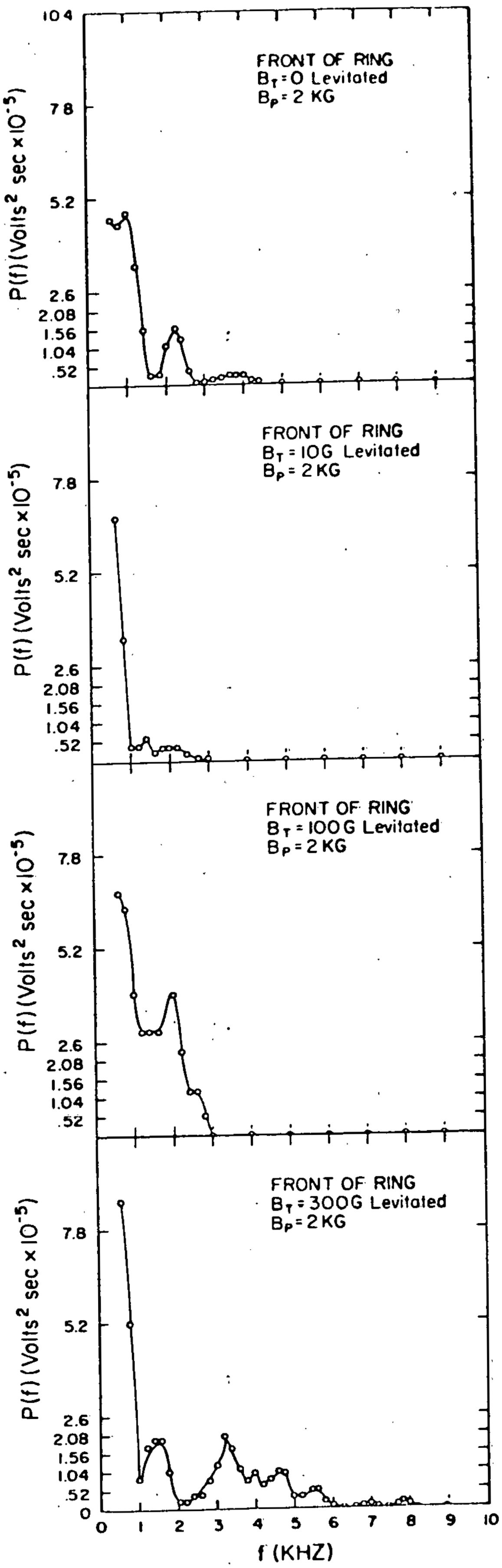
FRONT OF RING
B_T = 0 Levitated
B_P = 2 KG
FRONT OF RING
B_T = 10G Levitated
B_P = 2 KG
FRONT OF RING
B_T = 100G Levitated
B_P = 2 KG
FRONT OF RING
B_T = 300G Levitated
B_P = 2 KG
P(f) (Volts² sec × 10⁻⁵)
10.4
7.8
5.2
2.6
2.08
1.56
1.04
.52
0
0 1 2 3 4 5 6 7 8 9 10
f (KHZ)

Fig. 6

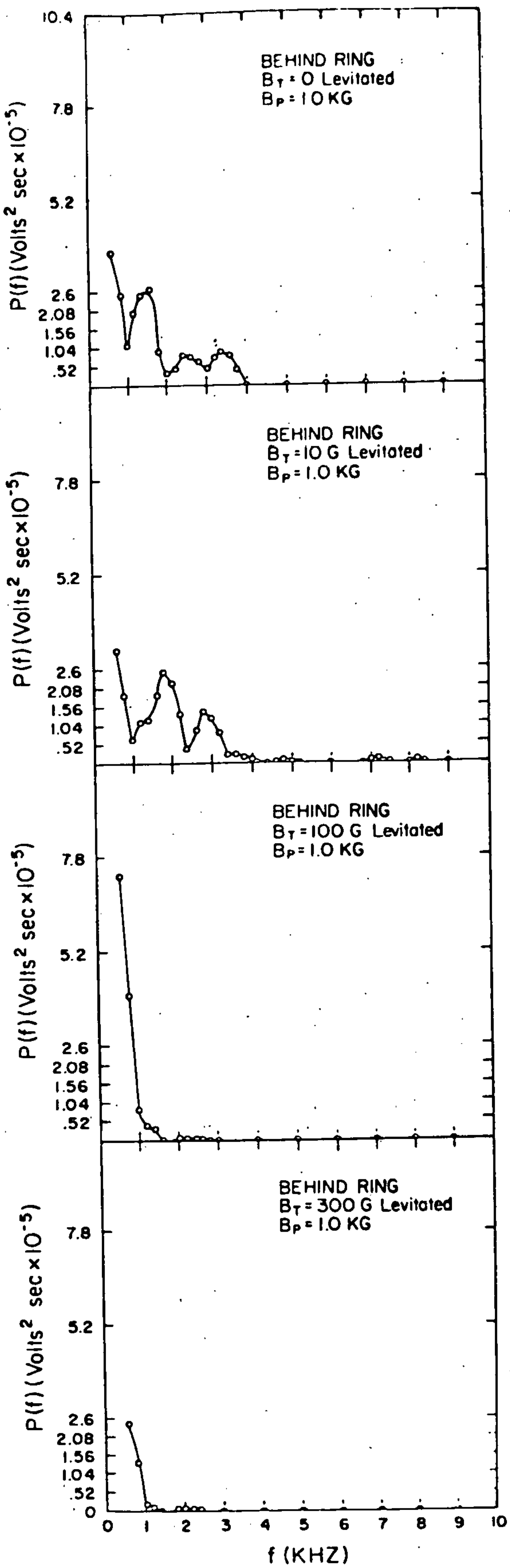
BEHIND RING
B_T = O Levitated
B_P = 1.0 KG
BEHIND RING
B_T = 10 G Levitated
B_P = 1.0 KG
BEHIND RING
B_T = 100 G Levitated
B_P = 1.0 KG
BEHIND RING
B_T = 300 G Levitated
B_P = 1.0 KG
P(f) (Volts^2 sec x 10^{-5})
10.4
7.8
5.2
2.6
2.08
1.56
1.04
.52
0
0 1 2 3 4 5 6 7 8 9 10
f (KHZ)

Fig. 7

EXTERNAL DISTRIBUTION IN ADDITION TO UC-20

R.W. Conn, University of California, Los Angeles
J.W. Flowers, University of Florida
H.S. Robertson, University of Miami, FL
E.G. Harris, University of Tennessee
M. Kristiansen, Texas Technical University
Plasma Research Laboratory, Australian National University
P.E. Vandplas, Association Euratom-Etat Belge, Belgium
P. Sananaka, Institute de Fisica-Unicamp, Brazil
A.M. Dupas, C.E.N.G., Dph-PFG-SIG, France
M.A. Loyau, Centre d'Etudes Nucleaires, France
G. VonGierke, Max-Planck-Institut Für Plasma Physic, Germany
R. Toschi, Associazione Euratom-Cnen Sulla Fusion, Cento Gas Ionizzati, Italy
K. Takayma, IPP Nagoy Imoversotu, Japan
K. Uo, Kyote University, Japan
K. Yamanto, JAERI, Japan
B. Lehnert, Royal Institute of Technology, Sweden
E.S. Weibel, CRPP, Ecole Polytechnique Federale de Lausanne, Switzerland
A. Gibson, Culham Laboratory, UK
R.S. Pease, Culham Laboratory, UK
D.R. Sweetman, Culham Laboratory, UK
J.B. Taylor, Culham Laboratory, UK
M.H. Hellberg, University of Natal, Durban, South Africa
Cheng-chung Yang, Chinese Academy of Sciences, Lanchow, Peoples Republic of China
Chi-shis Li, Chinese Academy of Sciences, Peking, Peoples Republic of China
Hsiao-wu Chêng, Chinese Academy of Sciences, Shanghai, Peoples Republic of China
Yi-chung Cho, Chinese Academy of Sciences, Peking, Peoples Republic of China
Fu-chia Yang, Futan University, Peoples Republic of China
Mei-ling Yeh, Chinese Academy of Sciences, Lanchow, Peoples Republic of China
Wei-chung Change, Chinese Academy of Sciences, Shanghai, Peoples Republic of China
Kuei-wu Wang, Chinese Academy of Sciences, Loshan County, Peoples Republic of China
Chûn-hsien Chên, Chinese Academy of Sciences, Peking, Peoples Republic of China
Li-tsien Chiu, Chinese Academy of Sciences, Peking, Peoples Republic of China
Miao-sun Chen, Chinese Academy of Sciences, Peking, Peoples Republic of China

6 for Chicago Operations Office
10 for individuals in Washington Offices

INTERNAL DISTRIBUTION IN ADDITION TO UC-20

100 for local group and file